

Two approaches to implementing projector–backprojector pairs for 3D reconstruction from Compton scattered data

Soo Mee Kim^a, Jae Sung Lee^{a,*}, Mi No Lee^b, Ju Hahn Lee^c, Chun Sik Lee^c,
Chan-Hyeong Kim^d, Dong Soo Lee^a, Soo-Jin Lee^b

^aDepartment of Nuclear Medicine and Interdisciplinary Program in Radiation Applied Life Science, Seoul National University, Seoul, Republic of Korea

^bDepartment of Electronic Engineering, Paichai University, Daejeon, Republic of Korea

^cDepartment of Physics, Chung-Ang University, Seoul, Republic of Korea

^dDepartment of Nuclear Engineering, Hanyang University, Seoul, Republic of Korea

Available online 10 November 2006

Abstract

Iterative image reconstruction for the Compton camera is computationally challenging since the projection and backprojection operations are performed on conical surfaces rather than along straight lines and there are many possible combinations of positions and energy measurements. Here, we note that implementing a computationally efficient projector–backprojector pair with good accuracy is an important factor to be considered in image reconstruction. In this study, two different approaches to conical surface integration were investigated for rapid calculations of projection and backprojection in 3D reconstruction; the ellipse-stacking method (ESM) and the ray-tracing method (RTM). Our experimental results indicated that while both methods produced equivalent reconstruction accuracies, RTM performed better than ESM in both computation time per iteration and total number of iterations for convergence.

© 2006 Elsevier B.V. All rights reserved.

PACS: 28.52.Av; S 29.40.–n; 28.41.Rc

Keywords: Compton camera; Projector; Image reconstruction; Emission tomography

1. Introduction

The Compton camera has been recognized as an innovative single-photon imaging device since, unlike the conventional single-photon imaging systems with mechanical collimators, it employs an electronic collimation based on the relationship between energy transfer and Compton scattering angle of γ rays in the detector. However, the Compton camera requires a fully three dimensional (3D) image reconstruction algorithm because the axial slice collimation is not used [1–3].

The 3D-expectation maximization (EM) algorithm based on the Poisson nature of radiation detection may be a choice for accurate reconstruction from Compton projection data. Iterative statistical reconstruction such as 3D-EM for the Compton camera is, however, computationally

challenging since the projection and backprojection operations are performed on conical surfaces rather than along straight lines, as in single-photon emission computed tomography (SPECT), and there are many possible combinations of positions and energy measurements. We note here that implementing a computationally efficient projector–backprojector pair with good accuracy is one of the most important factors to be considered in image reconstruction. In this work, two different approaches to conical surface integration were investigated for rapid calculations of projections and backprojections in 3D-EM reconstruction.

2. Methods

2.1. 3D-EM reconstruction for the Compton camera

A Compton camera system consists of two detectors, scatterer and absorber, which are parallel to each other as

*Corresponding author. Tel.: +82 2 2072 2938; fax: +82 2 745 7690.
E-mail address: jaes@snu.ac.kr (J.S. Lee).

shown in Fig. 1. A valid event is recorded when a photon is scattered in the first detector and then absorbed into the second detector. The following information is obtained for each valid event: (1) an interaction position in the scatterer, (2) an interaction position in the absorber, and (3) a scattering angle ω determined from the energy transferred to the scatterer.

For each combination of interaction positions in the two detectors and a scattering angle, the axis $\overline{P_1P_2}$, an apex P_1 and the half-angle ω of the conical surface are determined and the Compton projection data can be obtained by the conical surface integral with respect to the source distribution.

A mathematical expression for the Compton projection data (ignoring random coincidences) can be given as

$$g_{P_1P_2\omega} = \sum_{ijk} f_{ijk} H_{ijk}^{P_1P_2\omega} \quad (1)$$

where $g_{P_1P_2\omega}$ and f_{ijk} represent the Compton projection data and the source distribution, respectively. The system matrix $H_{ijk}^{P_1P_2\omega}$ represents the probability that a photon emitted from a voxel (i, j, k) is scattered at a position P_1 of the scatterer with a scattering angle ω and detected at a position P_2 of the absorber.

The EM algorithm, which is the same for all emission imaging systems is given by [4–6]

$$\hat{f}_{ijk}^{n+1} = \frac{\hat{f}_{ijk}^n}{\sum_{P_1P_2\omega} H_{ijk}^{P_1P_2\omega}} \sum_{P_1P_2\omega} H_{ijk}^{P_1P_2\omega} \frac{g_{P_1P_2\omega}}{\sum_{klm} \hat{f}_{klm}^n H_{klm}^{P_1P_2\omega}}. \quad (2)$$

The above EM algorithm is implemented by iterations requiring projection of the estimated source distribution and backprojection of the ratio between the measured and estimated projection data.

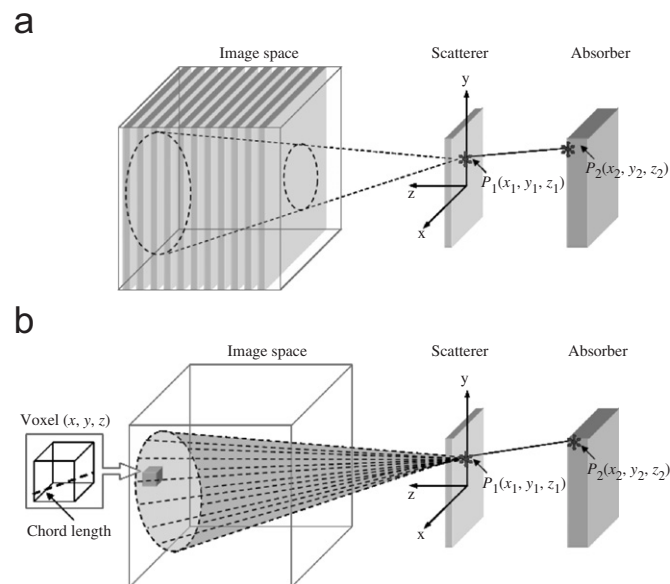


Fig. 1. The conical surface integral was calculated using two different approaches: (a) ellipse-stacking method and (b) ray-tracing method.

2.2. Two approaches for the system matrix

For efficient computation of the system matrix, it can be factorized into several sub-probabilities:

$$H_{ijk}^{P_1P_2\omega} = P_{ijk}^{P_1P_2\omega} P_{\omega}. \quad (3)$$

Elements for the system matrix were calculated by the product of the probability with which the voxel (i, j, k) belongs to a conical surface determined by P_1 , P_2 , and ω ($P_{ijk}^{P_1P_2\omega}$) and the probability relating to Compton scattering interaction on the scatterer (P_{ω}). If the interaction in the scatterer is only the Compton scattering, the probability P_{ω} is the differential cross-section for the Compton scattering that can be calculated with the Klein–Nishina formula with the assumption of electron at rest [7]. In this study, we considered two different approaches for rapidly calculating the belonging probability $P_{ijk}^{P_1P_2\omega}$; the ellipse-stacking method (ESM) and the ray-tracing method (RTM). For simplicity, we assumed an uniform distribution for probability P_{ω} .

The intersection of an x – y plane and a conical surface forms an ellipse. The ellipse equation can then be derived from the inner product of two vectors: $\overline{P_1P_2}$ and the vector from the voxel on the ellipse to P_1 . In ESM (Fig. 1(a)), the belonging probability was determined by the closeness of the neighboring voxel to the ellipse. The closeness was measured by the weights used in bilinear interpolation; each weight is inversely proportional to the distance from the existing sample point on the ellipse to a neighboring voxel.

In RTM (Fig. 1(b)), the belonging probability was determined by the intersecting chord length [8] of the voxel with a straight line passing through the apex of the cone along the conical surface.

2.3. Computer simulation

It was assumed that the Compton camera consisted of a pair of parallel scatterer and absorber with 16×16 detector elements with an active area of $5 \times 5 \text{ cm}^2$. The scattering angle of the incident photon at the scatterer was quantized into 30 discrete angles between 10° and 100° .

Two mathematical cylinder phantoms were used for simulation. Fig. 2(a) shows the phantom with three

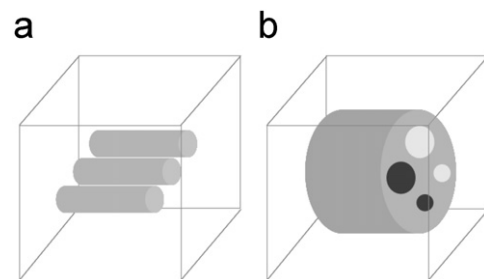


Fig. 2. Two mathematical phantoms: (a) 3-cylinder phantom and (b) 5-cylinder phantom.

cylinders of same diameter and activity. Fig. 2(b) shows the cylindrical phantom, which contains hot or cold inserts with different diameters and activities.

Projection data for the phantoms were generated using both ESM and RTM. The iterative 3D-EM reconstruction algorithms were also implemented using both ESM and RTM. Computation time and percent errors (PE, normalized root-mean squared errors) between the mathematical phantom and reconstructed images ($64 \times 64 \times 64$ matrix with pixel size of 1.56 mm) were compared.

3. Results

To compare the performance of the projector–backprojector pairs using ESM and RTM, EM reconstructions were performed with 64 iterations. Simple backprojection (SBP) reconstruction was also used for the comparison. Fig. 3 shows the central planes of the 3-cylinder phantom and the reconstructed images, which are parallel to the scatterer.

Fig. 4 shows the central profiles of the phantom and reconstructed images shown in Fig. 3 and the plots of percent errors versus iterations for EM reconstructions using RTM and ESM. The 3D-EM reconstructions clearly outperformed SBP in terms of the image contrast and spatial resolution. The EM reconstructions for the 5-cylinder phantom also shows good contrast between the inserts and background (Fig. 5) for both methods.

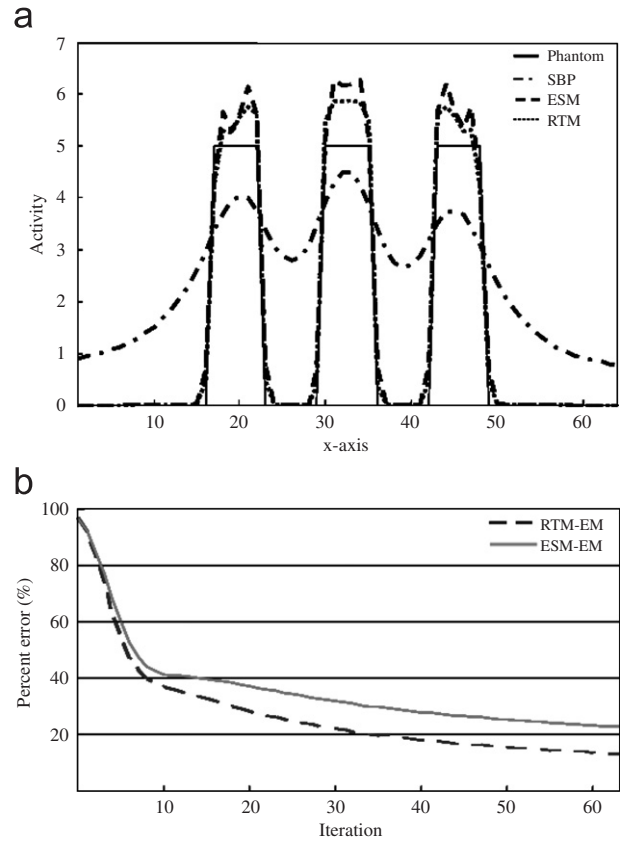


Fig. 4. Data for (a) central profiles and (b) convergence curve of percent errors.

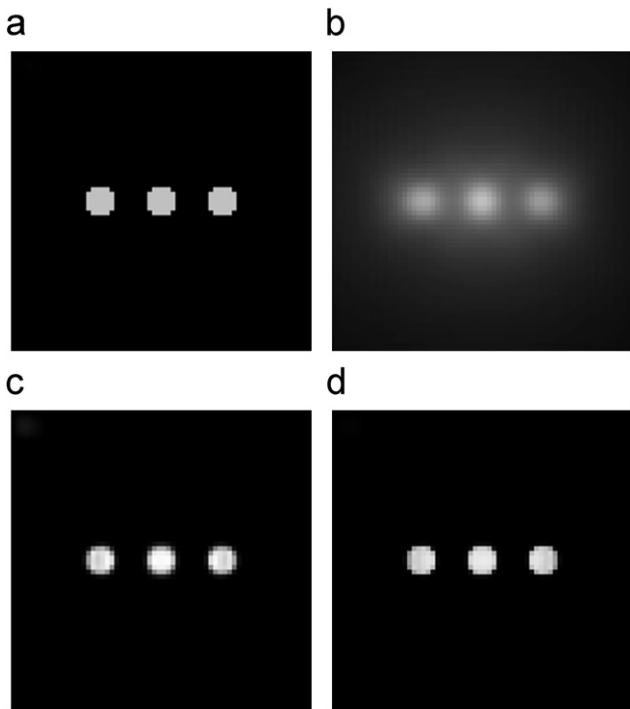


Fig. 3. The central planes parallel to the scatterer: (a) 3-cylinder phantom, (b) SBP (PE = 167.3%), (c) EM using ESM (22.7%) and (d) EM using RTM (13%).

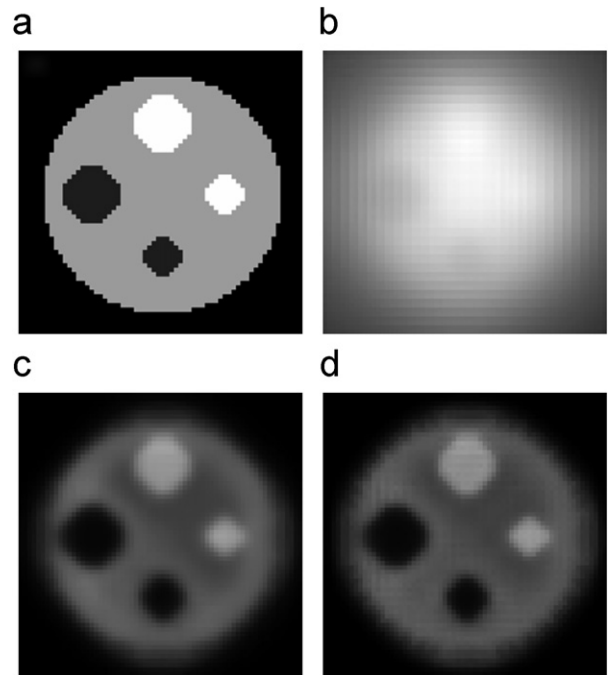


Fig. 5. The central planes parallel to the scatterer: (a) 5-cylinder phantom (b) SBP (612.1%), (c) EM using ESM (46.6%) and (d) EM using RTM (46.8%).

Although ESM produced comparable reconstructions to RTM, it required about three times longer computation time to converge.

4. Discussion and conclusion

Two different approaches to implementing projector–backprojector pairs for 3D-EM reconstruction from Compton projection data were investigated. Our experimental results showed that while the accuracies of reconstructions by both methods were equivalent, RTM performed better than ESM in both computation time per iteration and total number of iterations for convergence. Parallelization of projection and backprojection calculations and the use of geometrical symmetry along with an efficient caching scheme could greatly reduce the computation time for both methods.

Acknowledgments

This work was supported by grants from the Basic Atomic Energy Research Institute Program (M20508050000-05B0805-00000) and the Basic Research Program (R01-2006-000-10296-0) of the Korea Science & Engineering Foundation.

References

- [1] M. Singh, *Med. Phys.* 10 (1983) 421.
- [2] C. Sauve, A.O. Here, W.L. Rogers, S.J. Wilerman, N.H. Clinthorne, *IEEE Trans. Nuc. Sci.* NS-46 (6) (1999) 2075.
- [3] J. Smith, *Opt. Soc. Am. A* 22 (2005) 445.
- [4] L. Shepp, Y. Vardi, *IEEE Trans. Med. Imag.* MI-1 (1982) 113.
- [5] K. Lange, R. Carson, *J. Comput. Assist. Tomog.* 8 (1984) 306.
- [6] T. Hebert, R. Leahy, M. Singh, *J. Opt. Soc. Am. A* 7 (1990) 1305.
- [7] M.J. Cree, P.J. Bones, *IEEE Trans. Med. Imag.* 13 (2) (1994) 398.
- [8] R. Siddon, *Med. Phys.* 12 (1985) 252.